Competitive Hydrolytic and Elimination Mechanisms in the Urease Catalyzed Decomposition of Urea

ARTICLE *in* THE JOURNAL OF PHYSICAL CHEMISTRY B · SEPTEMBER 2007

Impact Factor: 3.3 · DOI: 10.1021/jp072323o · Source: PubMed

Competitive Hydrolytic and Elimination Mechanisms in the Urease Catalyzed Decomposition of Urea

Guillermina Estiu[†] and Kenneth M. Merz, Jr.*

Department of Chemistry and the Quantum Theory Project, 2328 New Physics Building, P.O. Box 118435, University of Florida, Gainesville, Florida 32611-8435

Received: March 23, 2007; In Final Form: June 15, 2007

We present a high-level quantum chemical study of possible elimination reaction mechanisms associated with the catalytic decomposition of urea at the binuclear nickel active site cluster of urease. Stable intermediates and transition state structures have been identified along several possible reaction pathways. The computed results are compared with those reported by Suarez et al. for the hydrolytic catalyzed decomposition. On the basis of these comparative studies, we propose a monodentate coordination of urea in the active site from which both the elimination and hydrolytic pathways can decompose urea into CO_2 and NH_3. This observation is counter to what has been experimentally suggested based on the exogenous observation of carbamic acid (the reaction product from the hydrolysis pathway). However, this does not address what has occurred at the active site of urease prior to product release. On the basis of our computed results, the observation that urea prefers the elimination channel in aqueous solution and on the observation of Lippard and co-workers of an elimination reaction channel in a urease biomimetic model, we propose that the elimination channel needs to be re-examined as a viable reaction channel in urease.

Introduction

The decomposition of urea is one of the most extensively studied chemical reactions.[1−6] There are several aspects of this reaction that have engendered long-term interest in this deceptively simple transformation. Among them, the competition between the hydrolytic and elimination pathways was an early focus of attention, with the hydrolytic pathway being preferred due to the exogenous observation of carbamic acid.[7−9] The hydrolytic mechanism, involving carbamate intermediates, has been proposed for the enzyme catalyzed reaction,[10−21] which ultimately yields CO_2 and NH_3 (see Scheme 1). However, these intermediates have been never found in the absence of the enzyme, neither in the aqueous phase nor in the presence of model binuclear nickel urease active site models.[22−24] Instead, cyanic acid intermediates have been detected, supporting an elimination mechanism that releases NH_3.[22−24] Moreover, the aqueous phase decomposition of urea prefers the elimination pathway over the hydrolytic one.[1,2] Taken together, the data suggests that the study of the elimination pathway in urease, while unpopular, deserves serious consideration and theoretical means provide the capability to provide insights into the likelihood of this pathway.

The kinetic parameters have been accurately determined for the aqueous phase elimination reaction,[1,2] but the determination for the uncatalyzed hydrolytic pathway has been hampered by the fact that the elimination reaction is much more facile than hydrolysis. Nevertheless, the rate constant has been recently proposed to be close to 10^{-11} from an extrapolation of the data derived from a kinetic study of tetramethylurea for which the elimination pathway is blocked.[25]

The relevance of this reaction is also related to its capability to model the reactivity of a peptide bond toward hydrolysis.[26−31]

SCHEME 1

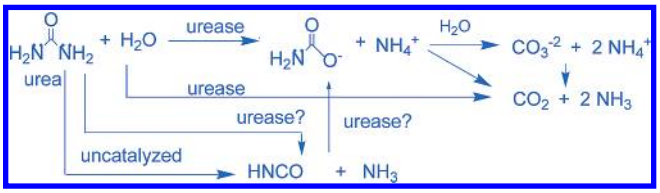

Because of this similarity, the proficiency of urease has been analyzed in comparison with that of other hydrolases.[25] The proficiency of an enzyme is defined as the relation of the rate constant of the enzyme-catalyzed process when the substrate concentration is low (k_{cat}/K_m) and the rate constant of the uncatalyzed reaction (k_{non}).[32−34] However, the mechanism of the enzymatic reaction has not been unambiguously determined, although it is known that the metalloenzyme urease catalyzes the conversion of urea 10^{14} times faster than the uncatalyzed elimination reaction.[16]

On the basis of biochemical studies and mutagenic experiments, Karplus et al.,[16] as well as Benini et al.,[17] have proposed hydrolytic mechanisms in which a water residue, coordinated to the binuclear Ni center of the active site, attacks the carbonyl carbon atom of the coordinated urea molecule (see Figures 1 and 2). The resulting tetrahedral intermediate collapses after the release of NH_3 to carbamate. The mechanisms proposed by both groups differ in the nature of the hydrolytic water, which can be a water molecule[16] coordinated to a single Ni ion or the OH bridging (so-called bridging-hydroxyl) between the two Ni atoms of the active site.[17] On the other hand, an elimination mechanism such as the one shown in Figure 3 has not been ruled out for the catalytic decomposition and needs to be reconsidered after the detection of cyanate intermediates in the reaction catalyzed by synthetic biomimetics.[22−24]

Understanding the mechanism of enzyme-catalyzed reactions is an important step in the design of so-called transition-state

* Corresponding author. E-mail: merz@qtp.ufl.edu.
[†] Current address: Department of Chemistry and Biochemistry, University of Notre Dame, Notre Dame, Indiana 46556.

10.1021/jp072323o CCC: $37.00
Published on Web 08/03/2007

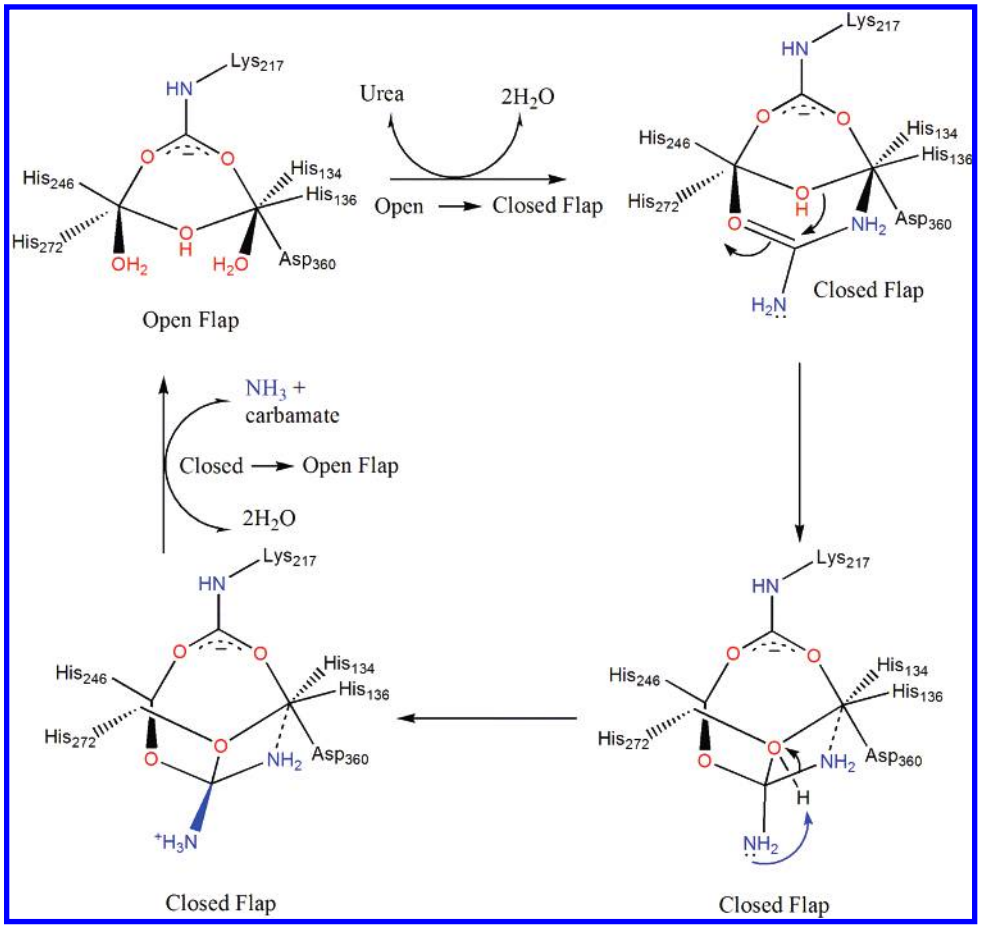

Figure 1. Structurally detailed mechanism for urease catalysis as proposed by Benini et al.[17] The reaction proceeds through a tetrahedral intermediate that gives carbamic acid after NH_3 release. The bridging OH acts as a nucleophile toward the carbonyl carbon and also protonates the free NH_2.

(TS) inhibitors. It is known that the most proficient enzymes are more sensitive to inhibitors that are designed to resemble presumed enzyme transition states due to the high binding energy of the TS-like structure(s).[33,35] Nevertheless, the proficiency of an enzyme cannot be determined before the mechanism is established because k_{non} corresponds to the uncatalyzed reaction that matches the catalytic pathway for which k_{cat}/K_m has been experimentally determined. In the case of urease, the problem is twofold: the mechanism of the enzyme-catalyzed reaction is not fully understood (defining an uncertainty in the reaction associated with k_{cat}/K_m) and for the solvent phase hydrolysis k_{non} has not been uniquely determined. Hence, by using the k_{cat}/K_m determined by Karplus, Pearson, and Hausinger (1.4×10^6 M^{-1} s^{-1} at 310.15 K),[16] an elimination mechanism results in a proficiency of 10^{13} ($k_{non} = 2 \times 10^{-7}$ s^{-1} at 333.15 K, from experiment),[2] whereas values of 10^{17} have been estimated from the experimental study of the hydrolysis of tetramethylurea.[25] Quantum chemical calculations have been also performed for the noncatalyzed hydrolysis,[36] resulting in a value that largely differs from the experimental one, thereby leading to a debate in the related literature.[37,38]

In addition to experimental studies, the urease-catalyzed decomposition of urea has been analyzed by means of modern theoretical methodologies. The hydrolytic reaction has been studied in cluster models of the active site, defined by the first coordination shell of the binuclear nickel metallocenter. At the B3LYP-LAPCVP level, activation free energies close to 30 kcal/mol have been calculated.[39] On the other hand, recent molecular dynamic simulations, which simultaneously modeled the three active sites of the trimeric structure in a single MD run, provide configurations that could be argued to proceed via either the hydrolytic and elimination pathways, suggesting a possible competition between these reaction mechanisms.[40] Taken in their entirety, these observations lend additional support to the elimination mechanism proposed in the early 1920s,[41,42] which has been recently reconsidered by Lippard and co-workers.[22−24] Hence, additional work toward identifying the elimination pathway is justified based on the accumulated experimental and computational observations.

We report in this article the results of extensive ab initio calculations of the enzyme-catalyzed elimination mechanism. Because of the dependence of the calculated free energies of activation on the computational model, we compare the hydrolytic and elimination mechanisms using the same cluster models and the same level of quantum mechanical theory. Merging the results of the present effort with that of Suarez et al.[39] for the hydrolytic decomposition provide us with a full QM description of the enzyme-catalyzed reaction.

Methodology

According to X-ray absorption spectroscopy (XAS) data, urease contains two pseudo-octahedral Ni(II) ions bound to *five* or *six* (N,O) donors at an average Ni−ligand distance of 2.06 Å.[43] Magnetic susceptibility experiments indicate that, in *jack bean* urease, the high-spin nickel(II) ions ($S = 1$) are octahedrally coordinated and have a weak antiferromagnetic coupling characterized by a J coupling constant of only -6.3 cm^{-1}.[44] The antiferromagnetic coupling of the bridged dinickel(II) systems has been experimentally determined for μ-acetate complexes[45] and theoretically evaluated for model systems of the urease active site.[39] The computational study of open-shell

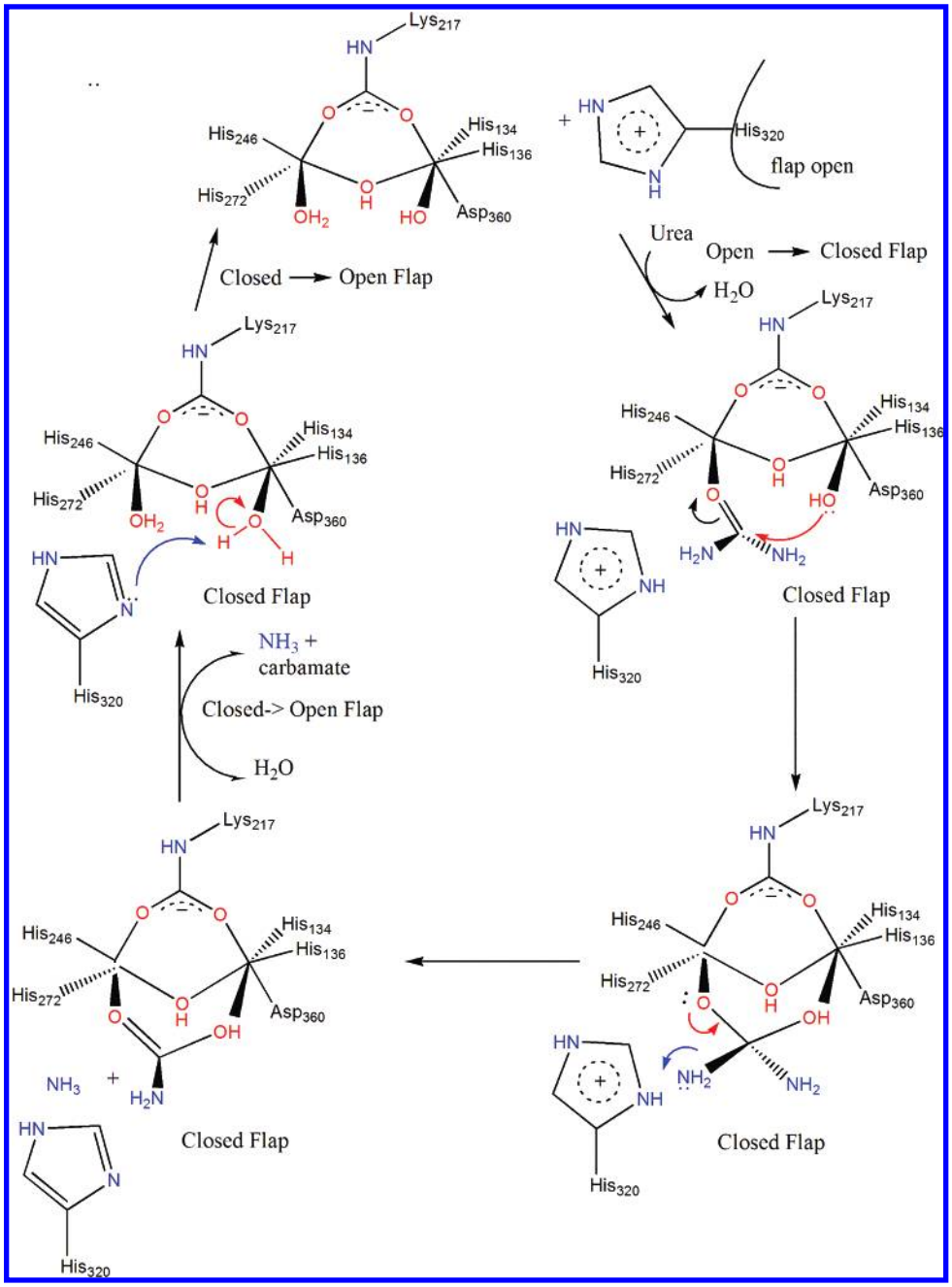

Figure 2. Structurally detailed mechanism for urease catalysis adapted from Karplus and Hausinger.[16] The reaction proceeds through a tetrahedral intermediate that gives carbamic acid after NH_3 release. It is based on the assumptions that (1) a water molecule is retained after urea coordination and that (2) His320 is protonated.

transition metal complexes can be efficiently carried out using the density functional theory (DFT) methods implemented in Gaussian 03.[46] In particular, the dinuclear systems studied herein were subjected to energy minimizations using the B3LYP functional[47] with the 6-31G* basis set[48] for nonmetal atoms and the Los Alamos effective core potentials (LANL2DZ)[49−51] for the metal atoms (this mixed basis set will be denoted as LACVP*). The use of effective core potentials for Ni ions has been previously calibrated by comparing the geometries, energies, and charges for a series of Ni−L complexes (L = OH^-, H_2O, CH_3COO^-, etc.) by using the LACVP*, 6-31G*, and 6-311G** basis sets for Ni.[39] Moreover, DFT methods have been shown to reproduce the structural properties of several biologically interesting transition metal centers, and their validity to model ground-state properties is widely accepted.[52−54]

The structures that are shown in this article are representative of the different steps involved in the postulated reaction pathways and have been fully optimized without imposed constraints. We report the structural parameters and associated energies for reactants, products, stable intermediates, and transition states. The search for stationary points on the potential energy surface utilized gradient-based algorithms and quadratic synchronous transit (QST2) approaches. Critical points have been further characterized by analytical computation of the harmonic frequencies at the same level of theory. A thermochemical analysis has been performed as a way to evaluate the free energy changes associated with the reaction, and solvent effects (aqueous solution) were included using an isodensity continuum polarizable model using standard settings within Gaussian.[55]

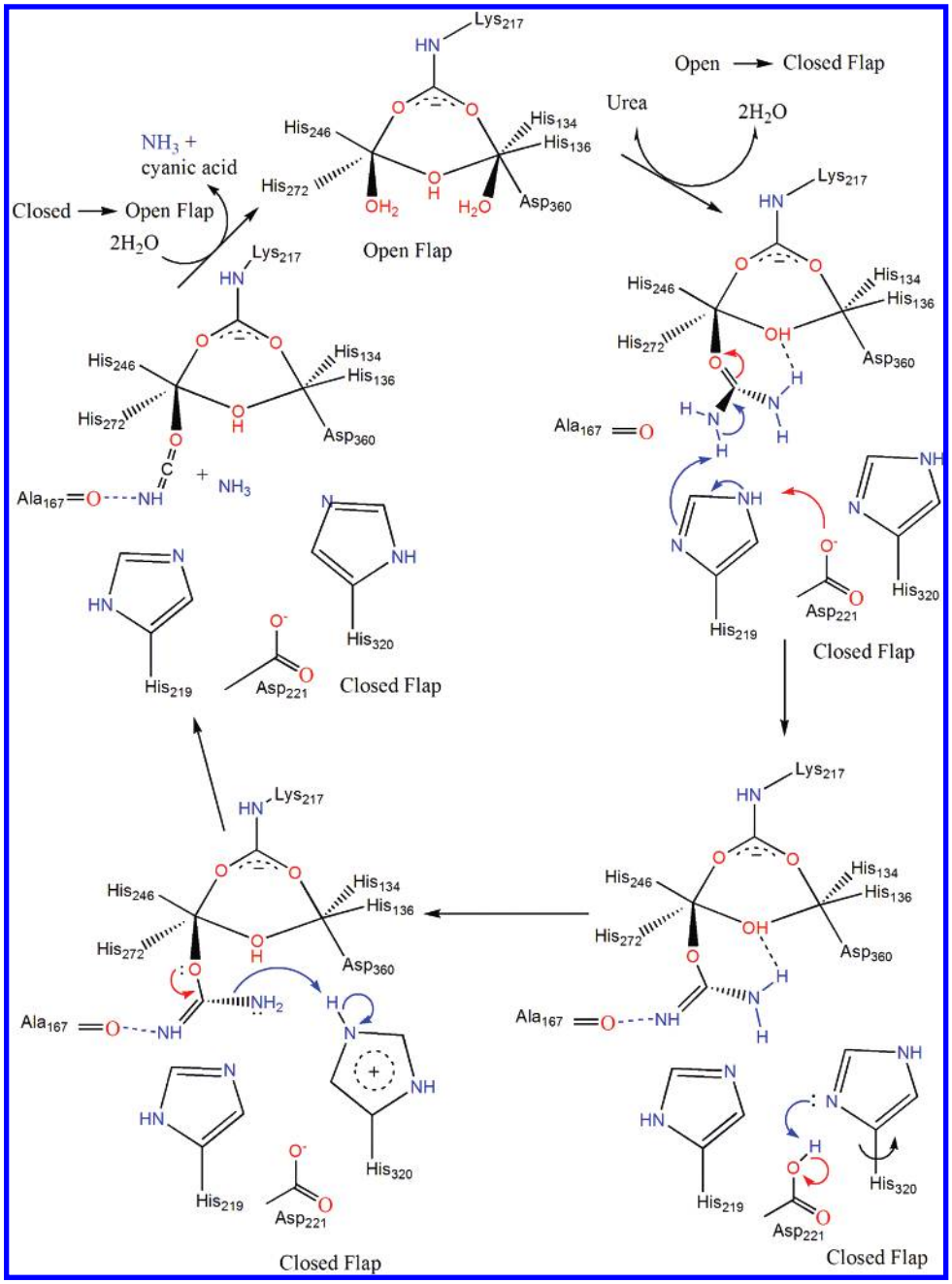

Figure 3. Structurally detailed mechanism for the proposed elimination pathway for urease-catalyzed urea decomposition.

The cluster models have been chosen to accurately reproduce the experimental parameters (crystallographic bond distances and angles). In the modeling using solvent, we have considered that, in enzymatic reactions, a ligand approaches the substrate from an aqueous environment and is surrounded by a biological environment when coordinated to the active site. On the basis of this concept, we have modeled the aqueous media for the approaching ligand and reaction products, and the biological environments were modeled without solvent influence for the active site clusters. In this way, we can qualitatively incorporate the effect of solvent on ligand binding and product disassociation, while treating the complexed structures as being in a medium of lower dielectric.

Results

Geometry of the Active Site. The structure of the native enzyme has been determined by X-ray crystallography at 2.0 Å resolution. The X-ray crystal structures of the native urease from *Kleiella aerogenes*[16,56] and *Bacillus Pasteurii*,[20,21] as well as subsequent crystallographic work based on mutagenesis experiments,[13−15,57] have identified a pair of nonequivalent Ni atoms at a Ni−Ni separation of ∼3.5 Å. Each Ni ion is coordinated to two histidine residues from the protein, and a carbamylated lysine bridges the two metal atoms (Figure 4). An aspartate residue further ligates the second nickel ion. Two terminally coordinated water molecules (W1, W2) and one bridging hydroxide ion (WB) complete the coordination sphere of the metal ions, resulting in a distorted square pyramidal (SP) environment for Ni(1) and a pseudooctahedral (Oh) one for Ni-(2). An additional water molecule (W3) forms strong H-bond contacts with WB, W1, and W2, defining a tetrahedral electron density distribution in the omit maps. While this tetrahedral shape has been determined for native *Bacillus Pasteurii*, the active-site water structure varies greatly between species,

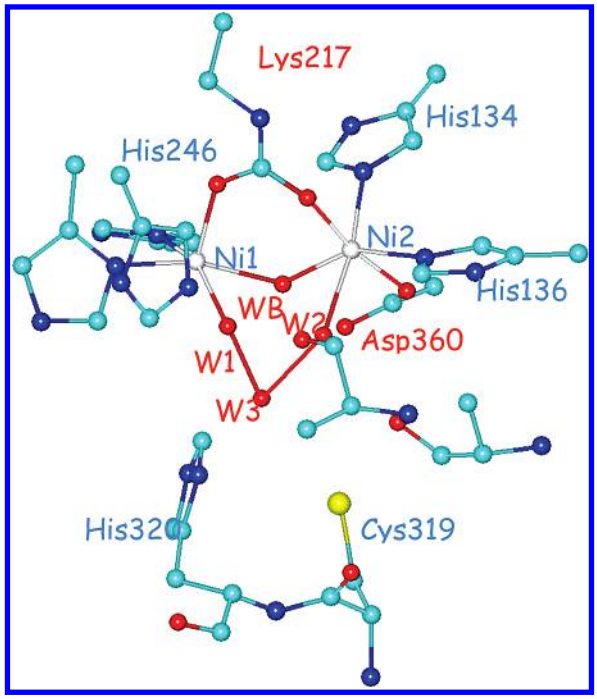

Figure 4. Active site of the binuclear nickel urease enzyme from *Klebsiella aerogenes* (PDB code 1FWJ) determined by X-ray crystallography. Relevant residues of the mobile flap are also shown. In all figures, O is red, N is blue, C is blue-green, S is yellow, and Ni is gray

reflecting its sensitivity to sequence differences and changes in the temperature of the X-ray experiments.[16] The water molecules of the active site are also important for establishing contacts with other conserved residues of the protein.[16,17,19] In addition to the variability of the active site solvent structure, there is a mobile flap, consisting of residues 308−337, that has been found in both open and closed conformations.[16−19,21] The mobility of the flap has been proposed to be important for regulating both the access of the substrate to the active site and the release of the reaction products. Moreover, the closed conformation is relevant for catalytic activity because it positions active site residues to interact favorably with the bound urea.

The experimentally determined geometry of the active site is retained after QM optimization (see S1, Figure 5), provided the X-ray coordinates are used as the starting geometry. However, in agreement with the observed mobility of the water molecules of the active site, we have found two additional minima (S2, S3, Figure 5) that differ in the coordination arrangement of the water molecules. The optimized structures (S1−S3) can be readily interconverted. Hence, the water molecule W3 can migrate to occupy the vacant site on Ni1, producing two octahedral Ni centers (S2, Figure 5). From this structure, which is isoenergetic to S1, either W1 or W3 can migrate back to the site originally occupied by W3. The migration of W3 restores the original structure (S1), while the migration of W1 results in structure S3, where the Ni-coordinated water molecule is opposite to the carbamylated Lys. This structure is 3 kcal/mol higher in energy than the X-ray structure.

From the superposition of S1 and S3 with the active site structure of the native enzyme (see Figure 6), it becomes evident that the first geometry (S1, Figure 5) is the one that best resembles the X-ray structure. Nevertheless, the possible reorganization of the active-site solvent structure has to be accounted for in the analysis of the catalytic mechanism. This reorganization is also supported by recent results from MD simulations, which show that both the migration of W3 to the vacant site in Ni1, as well as its exchange with other solvent−water molecules, is favored at room temperature.[40]

Geometry of the Urea-Coordinated Complex. The different structural properties of both Ni centers suggest different mechanistic roles for the two metal atoms. There is general agreement that the role of the square pyramidal Ni1 center is to bind urea via the carbonyl oxygen of urea. The second Ni atom has been suggested to help the catalytic pathway in different ways, either providing a solvent molecule as a nucleophile[16] or coordinating an amino group of the urea molecule.[17] The coordination of an amine group to Ni2 generates a bidentate mode that resembles the structure determined by X-ray crystallography for DAP (DAP = diamidophosphate)[17] and $B(OH)_3$ inhibited urease.[18] These structures have been proposed to mimic the transition state and substrate found in the hydrolytic mechanism, featuring the closed and open conformations of the mobile flap, respectively.[17,18] Nonetheless, the single-coordination mode has been found to be more stable according to high-level QM calculations,[39] although no inhibitor has been found that models this coordination mode.

All the possible coordination modes of urea need to displace water molecules from the active site. The simplest coordination mode involves urea occupying the vacant site of the pentagonal Ni2 center, only releasing W3. The complex that results from this binding mode (S1uw, Figure 5), features two Ni centers of octahedral symmetry and is found to be 5 kcal/mol less stable than the separated species. The same coordination process can start with S3 instead of S1, resulting in two Ni sites of octahedral symmetry. This structure (S3uw, Figure 5) is 7 kcal/mol higher in energy than the separated species. In both cases, urea binds to Ni through its carbonyl group (O−Ni = 2.24 and 2.22 Å in S1uw, S3uw, respectively), while one amino end of urea has a strong hydrogen bond contact with the bridging hydroxide ($H(NH_2)$−O(WB) = 1.64 Å in both S1u and S3u). The remaining W2 water molecule also contributes to the binding of urea by establishing a hydrogen bond with one of the NH_2 groups (H(W2)−N = 2.04 and 2.26 Å in S1uw and S3uw, respectively). The positions of the rest of the Ni ligands are not significantly altered upon urea binding. Minor distortions in the planar angles of the Ni1 metal center are observed that can be associated with the change in symmetry from distorted square pyramidal to O_h. The Ni−Ni distance increases 0.06 Å after urea binding, from 3.53 to 3.59 Å in S1uw and from 3.57 to 3.63 Å in S3uw.

The release of either W1 (in S1uw) or W3 (in S3uw) restores the pentagonal symmetry on Ni1, which resembles the structure determined for native urease.[16−19,21,56] S1u is more stable than S1uw by 0.5 kcal/mol, while S3u is 5 kcal/mol more stable than S3uw. Hence, the resulting structures (S1u, S3u, Figure 5) are nearly isoenergetic. The release of W1 from S1uw does not trigger any change in the orientation of the ligands. The urea ligand in S3u is tilted toward the position previously occupied by W3 in S3uw, favoring the hydrogen bond coordination of the urea amide hydrogen with the bridging OH. The interatomic distances that characterize urea binding are the same as previously described for S1uw and S3uw; however, the Ni−Ni distance decreases, approaching the value found in the native urease cluster (3.55 and 3.49 Å in S1u and S3u, respectively). S3u can be thought as arising from the replacement of the water molecule at Ni2 by urea.

Urea binding can also displace the three water molecules of the active site by coordinating in a bidentate manner through the carbonyl oxygen and the amide nitrogen (see Figure 7). This

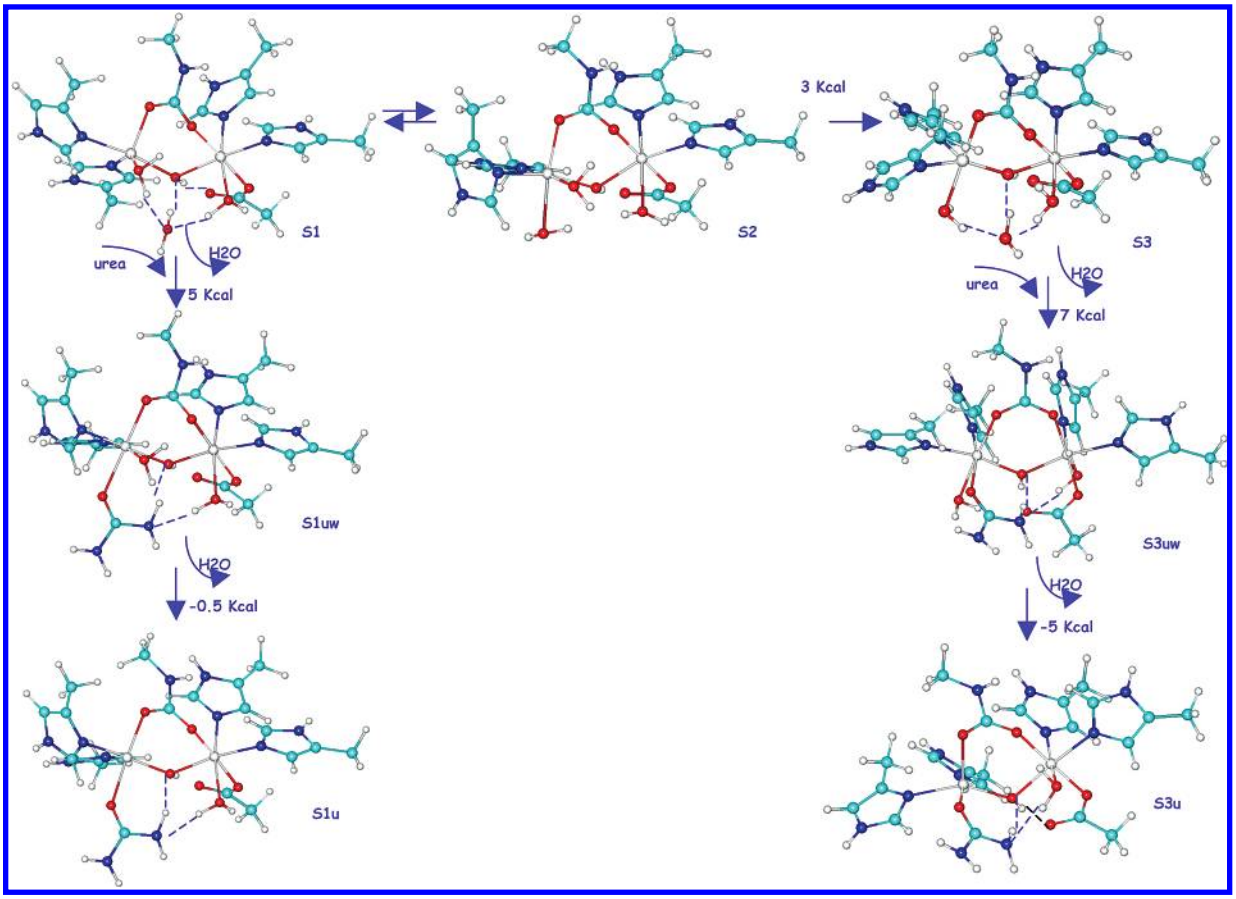

Figure 5. B3LYP-LAPCV optimized structure of the active site cluster models for the native enzyme (S1, S2, S3) and the urea-coordinated complexes (S1uw, S3uw, S1u, S3u). Free energy differences are given in kcal/mol.

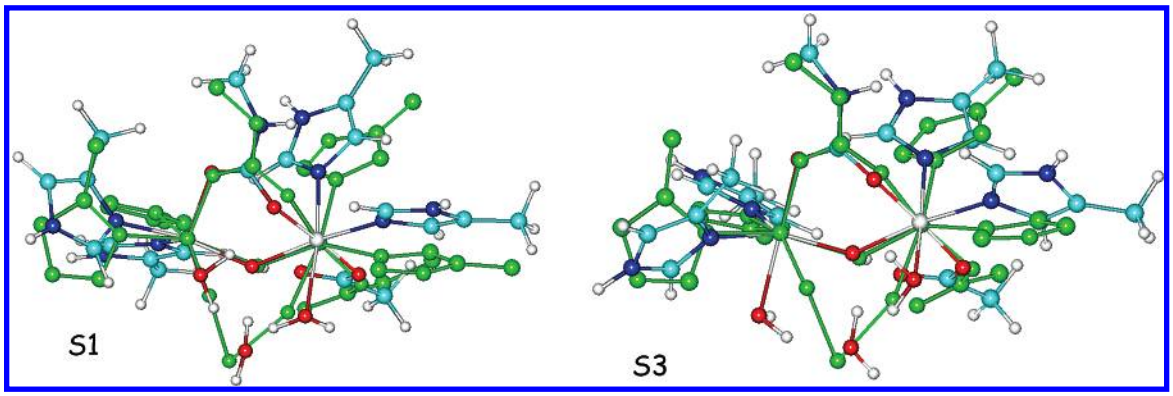

Figure 6. Superposition of the active site of the native enzyme (from *Klebsiella aerogenes*, pdb code 1FWJ, in green) and the optimized structures S1 and S3.

coordination mode has been proposed on the basis of the X-ray structure of DAP-inhibited urease (pdb code 3BPU).[17] The resulting complex has been found to be 6 kcal/mol higher in energy than the monodentate structure S3u.[39] Nonetheless, it has been proposed to be a reactive complex because it positions urea in an optimum orientation for a nucleophilic attack at the carbonyl carbon by the bridging OH.[39] From this coordination mode, only the hydrolytic pathway can be followed, whose energy profile has been already calculated and thoroughly described by Suarez et al.[39] It will be considered here only on a comparative basis.

Bidentate coordination keeps the octahedral symmetry of Ni2, although the coordination of NH_2 is in the position originally occupied by W2. Instead, the local symmetry of Ni1 is distorted from square pyramidal to a trigonal bipyramidal geometry (see

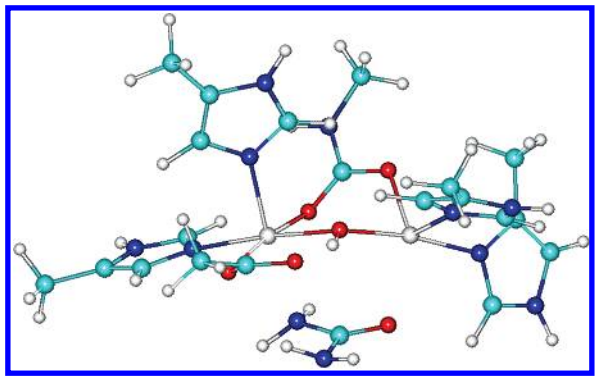

Figure 7. B3LYP-LAPCV optimized structure resulting from a bidentate coordination of the urea to the urease active site cluster.

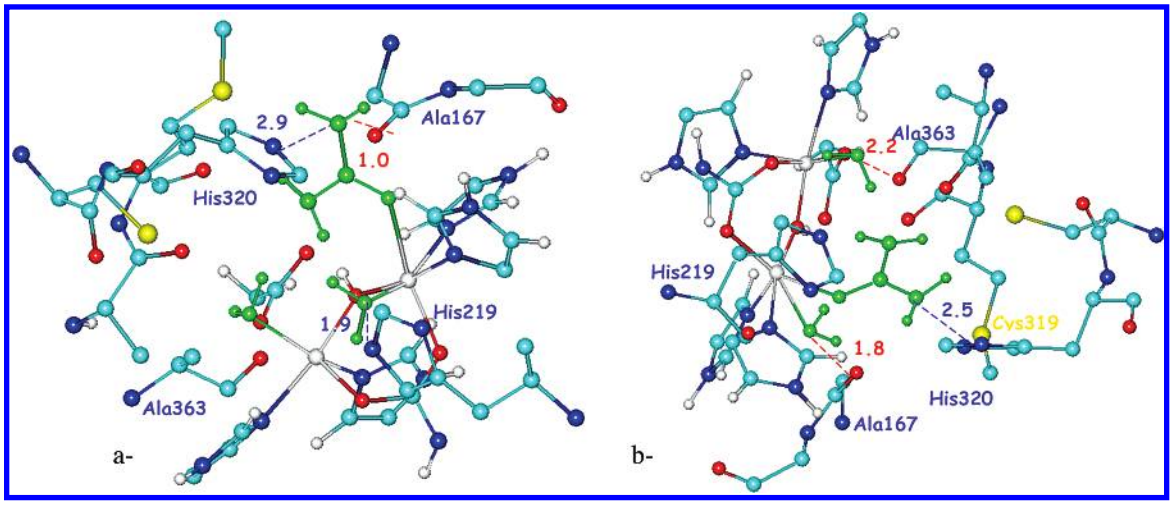

Figure 8. Docked structures of S1wu (a) and S3uw (b) within the 1FWJ X-ray structure (*K. aerogenes* residue numbering). Urea and the water molecules that are retained in the active site are shown in green. Select distances are given in Å. Further details are provided in the text.

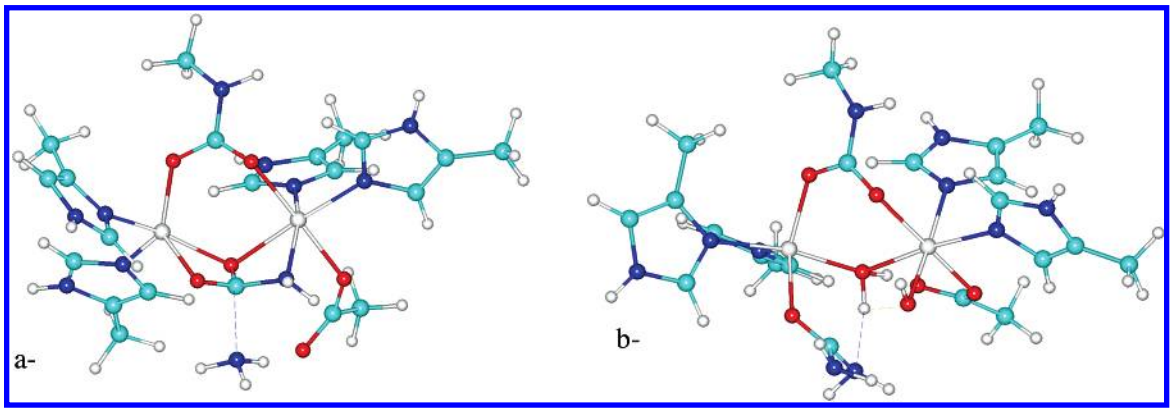

Figure 9. Transition state structures of the rate-determining step for the two proposed hydrolytic mechanisms.[39] Further details are provided in the text.

Figure 7). This symmetry change reflects a change in the molecular orbital pattern that may trigger an associated change in the multiplicity. For this reason, states of multiplicity 5 and 3 have been compared for all structures. The higher multiplicity has been found to be more stable in all cases by about 25 kcal/mol and, as a result, lower multiplicities will not been further considered.

In addition to the relative stabilities of the various cluster model structures, the ability of the different geometries to be accommodated by the protein environment has to be considered. Previous analyses, based on a rigid docking of the urea molecule into the "reactive" closed-flap structure of 1FWJ, have concluded that only the bidentate coordination is compatible with the closed conformation of the mobile flap. In particular, the monodentate geometry generates steric clashes between urea and the carbonyl group of Ala170.[39] To better evaluate the interactions that can be established between the active-site-bound urea and the protein environment, we have used a protein structure equilibrated at room temperature in the presence of an active-site model with urea bound in a bidentate manner into which we subsequently docked S1uw and S3uw into the active site pocket. The equilibration was done as part of a series of MD simulations (using Amber 8),[58] in which the urea-docked structure was built from the crystallographic coordinates of 3BPU.[40] Figure 8 shows how the urea molecule, in S3uw, fits in the protein environment, clearly favoring the formation of favorable interactions with nearby active site residues. In particular, the interactions with His320 and His219 (whose imidazole nitrogen is oriented toward the carbonyl oxygen of urea) are clearly present and are generally accepted to play significant roles in the catalysis.[16,17] For the same structure, the water molecule bound to Ni1 is close to the carbonyl oxygen of Ala167. Although this contact can be easily avoided by a slight modification of the Ni1−O(W1) bond orientation, it may indicate a preference for S3u instead of S3uw. The docking study of S1uw, on the other hand, shows that this coordination mode is sterically hindered by close contacts with the carbonyl group of Ala170.

Competitive Mechanisms Starting from the Monodentate Complex. The urease-catalyzed decomposition of a monodentate urea molecule can proceed through hydrolytic or elimination pathways. The mechanism of the hydrolytic decomposition has been analyzed by Suarez et al.[39] for the mono- and bidentate coordination modes, and similar activation energies (close to 31.5 kcal/mol) have been calculated in both cases. For the hydrolysis of bidentate urea, the rate-determining step is associated with the release of NH_3 from a transition state structure where the urea carbon atom is bound to the bridging oxygen atom (O(WB)) (see Figure 9a). This mechanism closely resembles the one proposed by Benini et al. (see Figure 1) and can only proceed from bidentate coordination of urea in the active site. A much simpler mechanism was found for the hydrolysis of monodentate urea, where the energy barrier is determined by the transfer of a proton from W2 to WB, forming a bifurcated hydrogen bond with the donor and acceptor atoms O(W2)−H (2.38 Å) and N(urea)−H (1.81 Å), respectively (see Figure 9b).[39] This proton transfer activates W2 for nucleophilic attack at the carbonyl carbon of urea.

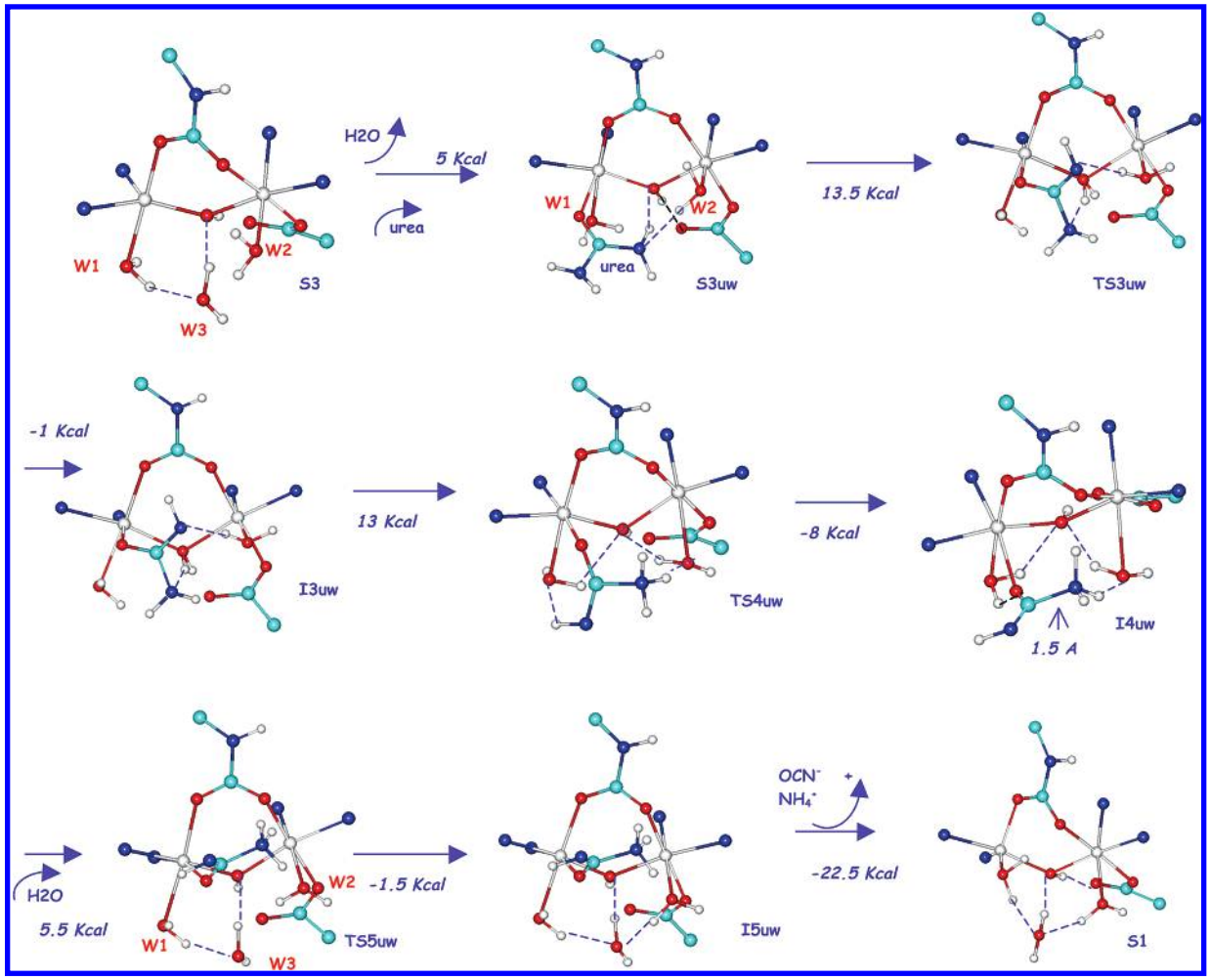

Figure 10. Energy profile for urea decomposition following an elimination mechanism starting at the monodentate complex S3. Free energy differences (kcal/mol) are reported for the different steps and were calculated at the B3LYP-LAPCV level of theory. The active site ligands have been simplified to increase the clarity of the figure.

Herein, we are focusing on the potential energy surface for the catalyzed decomposition of urea that follows an elimination pathway rather than hydrolysis. Although the coordination to S1 to give S1uw is energetically favored in the model clusters, the docking analysis leads us to conclude that S3uw is the best initial geometry for the active site. In S3uw, urea is perpendicular to Lys217 and is oriented in the same direction as the water molecule bound to Ni2 (see Figure 5). This coordination mode favors interactions with W2, which can stabilize intermediates and transition states along the reaction pathway. After the coordination of urea to S3, the reaction can proceed through S3uw, keeping W1 in the intermediate steps of the reaction, or through S3u, with the release of W1 as the first step of the reaction pathway. The corresponding reaction pathways are shown in Figures 10 and 12, respectively.

In S3uw (Figure 10) the acidity of the amide nitrogen of urea is increased by an acceptor hydrogen bond interaction with W2 (H(W2)−N = 1.67 Å). Similarly, a hydrogen bond interaction with Asp360 is responsible for the augmented nucleophilicity of WB (H(WB)−O(Asp) = 1.69 Å). These combine to facilitate the transfer of a NH_2 proton from urea to WB, giving the TS, TS3uw, in which the deprotonated NH of urea is stabilized by a hydrogen bond with W2 (H(W2)−N = 1.67 Å). An additional stabilizing interaction is a hydrogen bond between the nitrogen atom of the other amide nitrogen and WB (N(urea)−H(WB) = 1.93 Å), while the hydrogen atoms of W1 are also at hydrogen-bonding distance with the urea carbonyl oxygen (H(W1)−

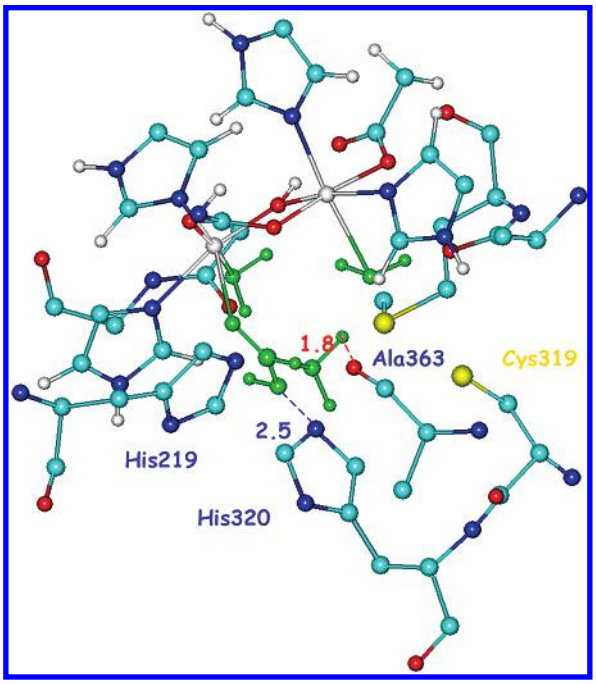

Figure 11. Docked structure of I4uw within the 1FWJ X-ray structure (*K. aerogenes* residue numbering). Urea and the water molecules retained in the active site are shown in green. Select distances are given in Å. Further details are given in the text.

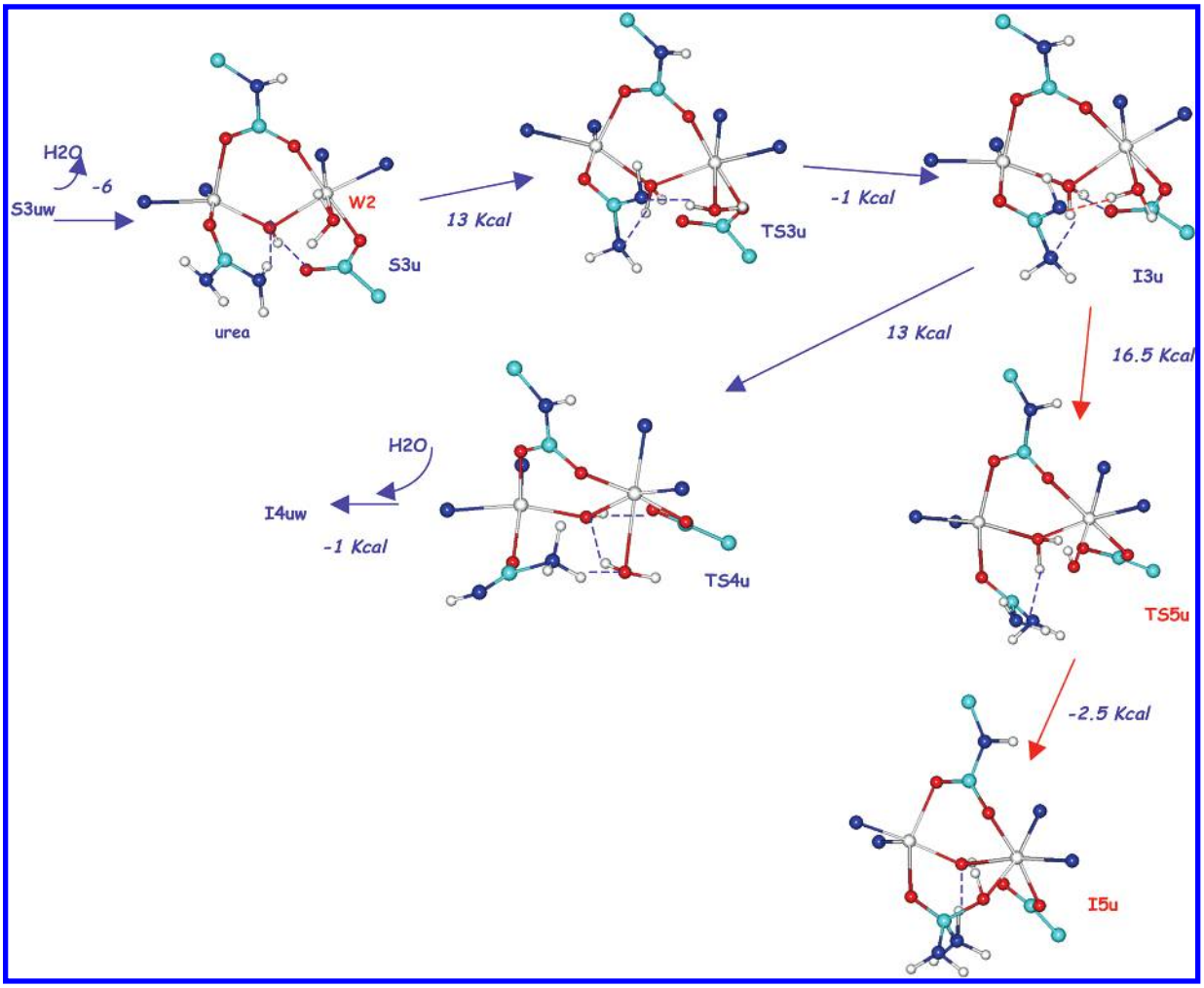

Figure 12. Energy profile for urea decomposition following an elimination mechanism starting at the monodentate complex S3 but releasing a water molecule after urea binding. Free energy differences (kcal/mol) are reported for the different steps and were calculated at the B3LYP-LAPCV level of theory. A competitive hydrolytic mechanism is indicated with red arrows. More details are provided in the text.

O(urea) = 1.82 Å). The transition-state structure (TS3uw) readily forms a stable intermediate (I3uw, see Figure 10). The next step of the reaction involves transfer of a proton from WB to the NH_2 of urea, resulting in TS4uw, which features an elongated bond between the carbon atom of urea and the protonated amide nitrogen that is a characteristic of the elimination mechanism (N(NH_3)—C(urea) = 1.57 Å), which results in the release of NH_3 leaving isocyanic acid (see Figure 10). This proton-transfer triggers a reorganization of the H-bond interactions, consistent with changes in the acid−base characteristics of the active site residues: W1 and W2 establish donor interactions with WB (H(W1)—O(WB) = 2.13 Å and H (W2)—O(WB) = 1.59 Å), and acceptor interactions from the protonated and deprotonated amide nitrogen atoms (H(NH_3)—O(W2) = 1.72 Å and H(NH)—O(W1) = 2.59 Å). After this rate-limiting step, intermediate I4wu is formed, which is stabilized by 8 kcal/mol relative to TS4uw by rearrangement of the hydrogen-bonding network. The last step begins the product release process and is facilitated by the addition of another water molecule to the hydrogen bond network associated with W1 and W2. This additional water restores the hydrogen bonding architecture characteristic of the active site of the native enzyme and facilitates the release of the products (NH_4^+ + NCO^-) through a disruption of the hydrogen bond interactions that stabilize the urea molecule in the active site. The resulting intermediate (I5wu) is close in energy with I4wu and proceeds through a TS, TS5uw, that is 4.5 kcal higher in energy than 14wu. The observed barrier can be partly attributed to the entrance of the water molecule into the hydrogen-bonding network of the active site. The release of the products restores the catalyst in the S1 configuration.

For the elimination mechanism of Figure 10, we calculate an activation free energy of 29.5 kcal/mol, 2 kcal/mol lower than the hydrolytic pathway. Besides the QM calculated energies, the protein environment can modulate the energy profile. The docking of I4uw into the protein active site shows that this intermediate can be further stabilized by hydrogen bond interactions with Ala363 and His320 (see Figure 11) when the mobile flap is in the closed conformation. Moreover, these residues could also guide the release of the products during flap opening.

An alternative reaction pathway proceeds via the release of W2 after (or simultaneously with) urea binding. This generates S3u, which is stabilized by 5 kcal/mol relative to S3uw (1 kcal/mol relative to reactants, see Figure 12). S3u favors proton transfer from the amide nitrogen of urea to WB (O(WB)—H(NH2) = 1.65 Å), by means of the hydrogen bond interaction of WB with Asp360 (H(WB)—O(Asp) = 1.68 Å). This proton transfer generates a TS structure (TS3u), which is 13 kcal/mol higher in energy, which has structural characteristics similar to TS3uw (H(W2)−N(urea) = 1.69 Å and N(urea)—H(WB) = 1.84 Å). TS3u easily evolves into a close-lying stable intermediate through reorientation of W1. Further proton transfer, via TS4u, to the NH_2 group of urea increases the free energy by 13

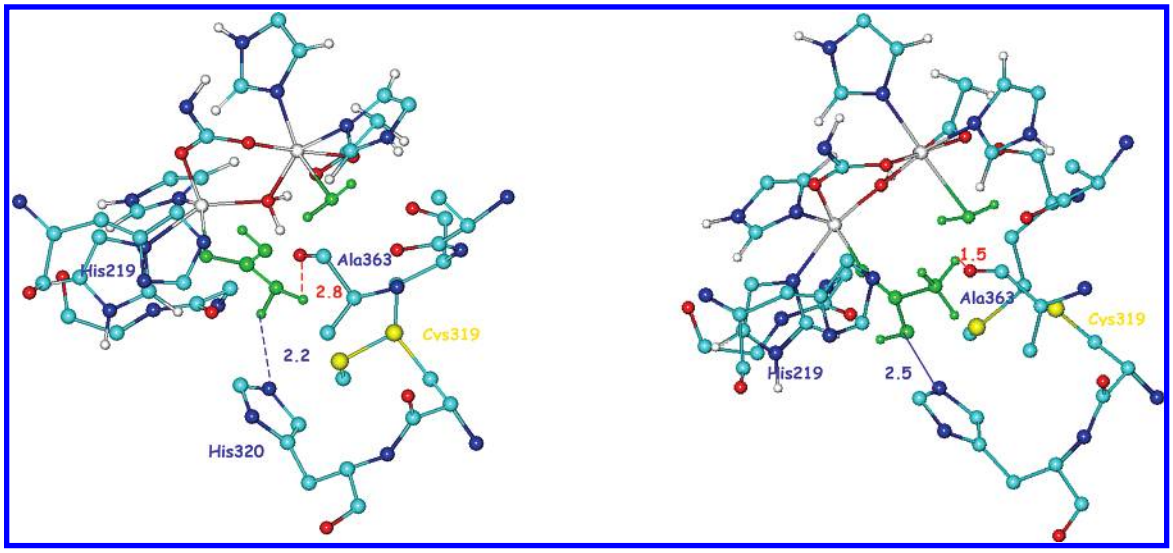

Figure 13. Docked structures of TS3u (a) and TS4u (b) within the 1FWJ X-ray structure (*K. aerogenes* residue numbering). The urea ligand and the water molecule that is retained are shown in green. Select distances are given in Å. More details are given in the text.

kcal/mol and defines the rate-limiting step. TS4u has structural features that are reminiscent of TS4uw (N—C(urea) = 1.54 Å, H(W2)—O(WB) =1.68 Å and (H(NH_3)—O(W2) = 1.84 Å). In the subsequent step, the system is stabilized via the coordination of an additional water molecule, which leads to intermediate I4uw, from which the subsequent steps follow those given in Figure 10. The activation free energy for this reaction pathway is 28.5 kcal/mol, only 1 kcal/mol lower than for the one given in Figure 10. Additional support for this alternative mechanism is provided via a docking analysis of S3uw, which suggested that the water molecule coordinated to the pentagonal site (W1) forms unfavorable contacts with Ala170 (see Figure 8), which are absent in S3u.

Stabilization of the reaction intermediates by the protein environment can also play a role in decreasing the activation energy of this reaction pathway. Figure 13 shows the interactions with Ala363 and His320 that could stabilize both TS3u and TS4u. These interactions may enhance the nucleophilicity of the NH_2 group in TS3u and assist the release of the reaction products in TS4u.

The comparison of the mechanisms shown in Figures 10 and 12 demonstrates that the coordination of water molecules in the last steps of the reaction facilitates product release and the restoration of the resting state of the enzyme. Moreover, in the first step of the reaction, the release of a water molecule stabilizes the urea-coordinated system. The calculated activation energies are, in both instances, very close to the one calculated for the hydrolytic mechanism. Hence, a definitive assignment of which reaction will be followed cannot be made. Instead, we propose that the hydrolytic and elimination mechanisms, by stint of their similar QM derived activation free energies, can be considered competitive with one another. It is noteworthy that the same conclusion was obtained from the analysis of MD simulations.[40]

For the elimination mechanisms analyzed in this article, the catalyst is restored after the reaction is completed. Hence, the same cluster structure models the active site before urea coordination and after product release. Therefore, the free energy of the reaction is determined by the difference in free energy between reactants (urea) and products (cyanic acid and ammonium). This energy difference has been calculated at the MP2/6-3111++G** (in the Figure 14 caption, 6-311++G** is used) level of theory,[36] showing that the products are present

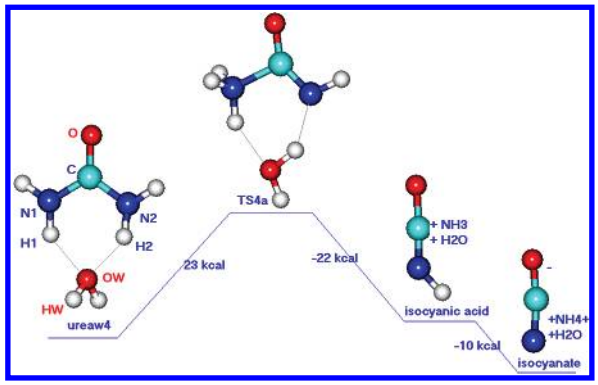

Figure 14. Reaction profile for the urea elimination pathway assisted by one water molecule, leading to isocyanic acid. ΔG_{act} values, calculated at the MP2/6-311++G** level, are solvent corrected.

as charged species (NH_4^+ and OCN^-) in an aqueous environment and are 5 kcal/mol more stable than the reactants using the IPCM approach to model solvent effects.[36]

In the mechanisms described above, the role played by the Ni1—Ni2 bridging hydroxide (WB) is of particular interest. WB acts initially as a base, accepting a proton from a NH_2 of urea. The pK_a of the resulting water-bridged residue is lowered by coordination to the positive metal ions and can easily transfer a proton to the remaining NH_2 group, helping in the release of NH_3. The mechanism can be described as a WB-assisted proton transfer rather than the water-assisted proton transfer previously described for the solvent phase elimination of urea (see Figure 14).[36] In addition to WB, W2 is also involved in the elimination mechanism in the enzyme-active site, helping to stabilize the NH end of urea after proton donation. This role is played by the catalytic water in the solvent-phase reaction but is hampered in the enzyme with respect to WB because the other hydrogen atom of WB is hydrogen bonded to Asp360.

A proton transfer from a bridging water molecule (between two nickel ions) to the NH_2 of Ni-coordinated urea has been found to have a low-energy barrier in the urease biomimetic complexes synthesized by Lippard and co-workers.[22−24,59] These inorganic complexes catalyze a similar elimination reaction involving the same steps but in reverse order: initial proton transfer from the bridging water molecule to a nitrogen atom of urea followed by proton donation from the other nitrogen atom to the bridging OH, a process that restores the catalyst's

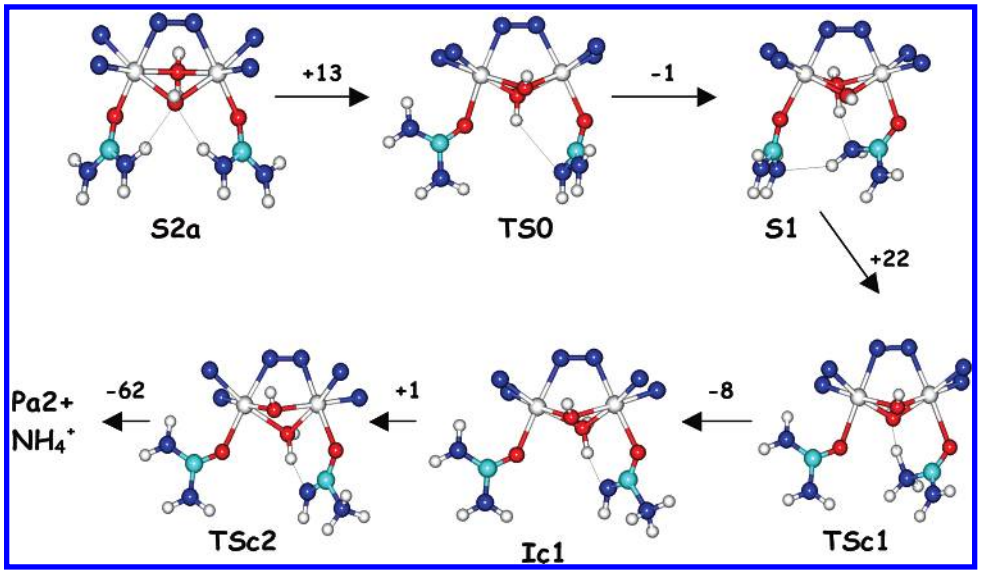

Figure 15. B3LYP/LACVP* optimized geometries of the intermediate (Ii), and transition state (TSi) structures involved in the elimination reaction proceeding through NH_3 release from the conformer S1. The aromatic phthalazine ligand has been deleted for clarity. Differences in the gas-phase free energy (ΔG) between consecutive steps are given.

structure (Figure 15). The water residue resembles the protonated state of WB in I3u (see Figure 9). The reaction mechanism has been discussed in detail by Estiu and Merz[59] and has an activation energy of 32 kcal/mol, calculated at the same level of theory as the one used in this research.

In addition to the wealth of QM-derived theoretical evidence that support elimination mechanisms for both the solvent phase and the catalyzed reaction, the results of MD simulations can be used to further support this reaction pathway. It has been found by Estiu and Merz[40]that the interactions stabilized during several 6 ns MD simulations indicate that a "protein-assisted" elimination mechanism is largely favored. In this mechanism, protein residues of the mobile flap mediate the transfer of a proton between the urea nitrogen atoms.[40]

At this stage, it is tempting to speculate that the enzyme-catalyzed reaction follows an elimination mechanism. However, the difference in the QM-derived free energies for the hydrolytic and elimination pathways is not large enough to justify this conclusion. Moreover, the relative probability for each mechanism to occur depends on a key reaction step that may follow different pathways: the conversion of I3u to TS4u (elimination) or to TS5u (hydrolysis, see Figure 12). The analysis of the hydrogen bond interactions that are established in I3u show that the proton transfer from the protonated bridging OH, WB, to the NH_2 moiety of urea may compete with a similar proton transfer from W2 to NH. The latter would proceed through TS5u and activate W2 for nucleophilic attack on the carbonyl carbon of urea, forming the tetrahedral intermediate characteristic of the hydrolytic pathway (I5u). The comparison of both reaction pathways shows that the rate-limiting TS structure for the hydrolytic mechanism is only 3.5 kcal/mol higher in energy than TS4u, corresponding to the elimination pathway. The role of W2, which can either transfer a proton to the deprotonated NH of urea or just stabilize it by hydrogen bond coordination, will determine the mechanism that will be followed. The relevance of this residue and the fact that S3u can fit in the protein environment without steric clashes, lead us to predict that this coordination is the one occurring in the urease active site, although no transition-state inhibitor structures have yet been found that mimic this coordination mode. Additional support for this prediction can be derived from MD simulations of the urease−urea system, starting from a model of the active site where the water molecule bound to Ni2 is retained. The results from these simulations would certainly complete those previously obtained from MD simulations starting from the bidentate complex of urea to the urease active site.[40]However, the theoretical and experimental data accumulated to date lead us to speculate that both mechanisms could compete in the enzyme-active site, ultimately leading to CO_2 and NH_3 after the hydrolysis of the corresponding intermediates.

Conclusions

In this work, we employ computational methodologies to analyze the energies involved in the catalytic decomposition of urea via either a hydrolytic or an elimination mechanism. The model complexes that we use, and their analysis at a high QM level, provide geometries, relative energies, and reaction pathways that allow one to address relevant biological questions surrounding the enzyme urease.

The characterization of the complex S3u, which nicely fits the protein environment presented by the closed-flap conformation of the enzyme, suggests that a Ni2-bound water molecule can be retained after urea coordination, and that it can actively participate in the reaction mechanism. Moreover, both the Ni—Ni bridging WB hydroxyl and the Ni2-bound water molecule play significant roles in both the hydrolytic and the elimination mechanisms.

The Ni−Ni separation is kept in all the TS and intermediates for both reaction mechanisms, and the two metal atoms preserve their coordination sphere. The largest structural modifications of the active site occur after coordination of urea in a bidentate manner. A reaction mechanism that proceeds through this structure will likely have a higher activation energy associated, in part, with the reorganization of the protein environment.

The results of our theoretical analysis of the urease-catalyzed decomposition of urea supports a reaction pathway that keeps a water molecule coordinated to the octahedral Ni center. We find that, within the errors our calculations, the hydrolytic and elimination mechanisms are equally favored and may compete in the enzyme-active site, ultimately leading to the final products: CO_2 and NH_3. Competitive mechanisms are frequently found for enzymatic reactions as a consequence of the complicated energy landscape associated with these biological pro-

cesses.[60] Moreover, these conclusions are in agreement with insights derived from MD simulations of the urea-coordinated urease system and are consistent with the available kinetic analysis of urease.[7,8,42,61] Future work will focus on the use of QM/MM approaches as well as comparison to experimental isotope effects[62] to further evaluate the relative merits of the classical hydrolytic pathway or the elimination pathway.

Acknowledgment. We thank the NIH for support of this research via GM066859. We also thank the NCSA and PSC for supercomputing support. We thank Bob Hausinger and Mo Cleland for help discussions concerning urease catalysis.

References and Notes

(1) Shaw, W. H. R.; Walker, D. G. *J. Am. Chem. Soc.* **1958**, *80*, 5337.
(2) Shaw, W. H.; Bordeaux, J. J. *J. Am. Chem. Soc.* **1955**, *27*, 4729.
(3) Laidler, K. J.; Hoare, J. P. *J. Am. Chem. Soc.* **1950**, *72*, 2489.
(4) Laidler, K. J.; Hoare, J. P. *J. Am. Chem. Soc.* **1950**, *72*, 2489.
(5) Langlois, S.; Broche, A. *Bull. Soc. Chim. Fr.* **1964**, 812.
(6) Dixon, N. E.; Gazzola, C.; Blakeley, R. L.; Zerner, B. *J. Am. Chem. Soc.* **1975**, *97*, 4131.
(7) Blakeley, R. L.; Hinds, J. A.; Kunze, H. E.; Webb, E. C.; Zerner, B. *Biochemistry* **1969**, *8*, 1991.
(8) Sumner, J. B.; Hand, D. B.; Holloway, R. G. *J. Biol. Chem.* **1931**, *91*, 333.
(9) Zerner, B. *Bioorg. Chem.* **1991**, *19*, 116.
(10) Musiani, F.; Arnolfi, E.; Casadio, R.; Ciurli, S. *J. Biol. Inorg. Chem.* **2001**, *6*, 300.
(11) Todd, M. J.; Hausinger, R. P. *Biochemistry* **2000**, *39*, 5389.
(12) Todd, M. J.; Hausinger, R. P. *J. Biol. Chem.* **1991**, *266*, 24327.
(13) Pearson, M. A.; Schaller, R. A.; Michel, L. O.; Karplus, P. A.; Hausinger, R. P. *Biochemistry* **1998**, *37*, 6214.
(14) Pearson, M. A.; Park, I.-S.; Schaller, R. A.; Michel, L. O.; Karplus, P. A.; Hausinger, R. P. *Biochemistry* **2000**, *39*, 8575.
(15) Pearson, M. A.; Michel, L. O.; Hausinger, R. P.; Karplus, P. A. *Biochemistry* **1997**, *36*, 8164.
(16) Karplus, P. A.; Pearson, M. A.; Hausinger, R. P. *Acc. Chem. Res.* **1997**, *30*, 330.
(17) Benini, S.; Rypniewski, W. R.; Wilson, K. S.; Miletti, S.; Ciurli, S.; Mangani, S. *Struct. Fold. Des.* **1999**, *7*, 205.
(18) Benini, S.; Rypniewski, W. R.; Wilson, K. S.; Mangani, S.; Ciurli, S. *J. Am. Chem. Soc.* **2004**, *126*, 3714.
(19) Benini, S.; Rypniewski, W. R.; Wilson, K. S.; Ciurli, S.; Mangani, S. *J. Biol. Inorg. Chem.* **2001**, *6*, 778.
(20) Benini, S.; Rypniewski, W. R.; Wilson, K. S.; Ciurli, S.; Mangani, S. *J. Biol. Inorg. Chem.* **1998**, *3*, 268.
(21) Benini, S.; Ciurli, S.; Rypniewski, W. R.; Wilson, K. S.; Mangani, S. *Acta Crystallogr., Sect. D* **1998**, *54*, 409.
(22) Barrios, A. M.; Lippard, S. J. *Inorg. Chem.* **2001**, *40*, 1250.
(23) Barrios, A. M.; Lippard, S. J. *J. Am. Chem. Soc.* **2000**, *122*, 9172.
(24) Barrios, A. M.; Lippard, S. J. *J. Am. Chem. Soc.* **1999**, *121*, 11751.
(25) Callahan, B. P.; Yuan, Y.; Wolfenden, R. *J. Am. Chem. Soc.* **2005**, *127*, 10828.
(26) Antonczak, S.; Ruiz-Lopez, M. F.; Rivail, J. L. *J. Am. Chem. Soc.* **1994**, *116*, 3912.
(27) Bakowies, D.; Kollman, P. A. *J. Am. Chem. Soc.* **1999**, *121*, 5712.
(28) Hine, J.; King, R. S.; Midden, R.; Sinha, A. *J. Org. Chem.* **1981**, *46*, 3186.
(29) Kallies, B.; Mitzner, R. *J. Mol. Model.* **1998**, *4*, 183.
(30) Krug, J. P.; Popelier, L. A.; Bader, F. W. *J. Phys. Chem.* **1992**, *96*, 7604.
(31) Slebocka-Tilk, H.; Sauriol, F.; Monette, M.; Brown, R. S. *Can. J. Chem.* **2002**, *80*, 1343.
(32) Garcia-Viloca, M.; Gao, J.; Karplus, M.; Truhlar, D. G. *Science* **2004**, *303*, 186.
(33) Wolfenden, R.; Snider, M. J. *Acc. Chem. Res.* **2001**, *34*, 938.
(34) Zhang, X. Y.; Houk, K. N. *Acc. Chem. Res.* **2005**, *38*, 379.
(35) Sievers, A.; Beringer, M.; Rodnina, M.; Wolfenden, R. *Proc. Natl. Acad. Sci. U.S.A.* **2004**, *101*, 7897.
(36) Estiu, G. L.; Merz, K. M., Jr. *J. Am. Chem. Soc.* **2004**, *126*, 6932.
(37) Editors' Choice. *Science* **2005**, *309*, 852.
(38) Estiu, G. L.; Merz, K. M., Jr. **2006**, manuscript in preparation.
(39) Suarez, D.; Diaz, N.; Merz, K. M. Jr. *J. Am. Chem. Soc.* **2003**, *125*, 15234.
(40) Estiu, G.; Merz, K. M., Jr. *Biochemistry* **2006**, *45*, 4429.
(41) Fearon, W. R. *Biochem. J.* **1923**, *17*, 84.
(42) Mack, E.; Villars, D. E. *J. Am. Chem. Soc.* **1923**, *45*, 505.
(43) Wang, S.; Lee, M. H.; Hausinger, R. P.; Clark, P. A.; Wilcox, D. E.; Scott, R. A. *Inorg. Chem.* **1994**, *33*, 1589.
(44) Clark, P. A.; Wilcox, D. E. *Inorg. Chem.* **1989**, *28*, 1326.
(45) Konrad, M.; Meyer, F.; Jacobi, A.; Kircher, P.; Rutsch, P.; Zsolnai, L. *Inorg. Chem.* **1999**, *38*, 4559.
(46) Frisch, M. J.; Trucks, G. W.; Schlegel, H. B.; Scuseria, G. E.; Robb, M. A.; Cheeseman, J. R.; Montgomery, J. A., Jr.; Vreven, T.; Kudin, K. N.; Burant, J. C.; Millam, J. M.; Iyengar, S. S.; Tomasi, J.; Barone, V.; Mennucci, B.; Cossi, M.; Scalmani, G.; Rega, N.; Petersson, G. A.; Nakatsuji, H.; Hada, M.; Ehara, M.; Toyota, K.; Fukuda, R.; Hasegawa, J.; Ishida, M.; Nakajima, T.; Honda, Y.; Kitao, O.; Nakai, H.; Klene, M.; Li, X.; Knox, J. E.; Hratchian, H. P.; Cross, J. B.; Bakken, V.; Adamo, C.; Jaramillo, J.; Gomperts, R.; Stratmann, R. E.; Yazyev, O.; Austin, A. J.; Cammi, R.; Pomelli, C.; Ochterski, J. W.; Ayala, P. Y.; Morokuma, K.; Voth, G. A.; Salvador, P.; Dannenberg, J. J.; Zakrzewski, V. G.; Dapprich, S.; Daniels, A. D.; Strain, M. C.; Farkas, O.; Malick, D. K.; Rabuck, A. D.; Raghavachari, K.; Foresman, J. B.; Ortiz, J. V.; Cui, Q.; Baboul, A. G.; Clifford, S.; Cioslowski, J.; Stefanov, B. B.; Liu, G.; Liashenko, A.; Piskorz, P.; Komaromi, I.; Martin, R. L.; Fox, D. J.; Keith, T.; Al-Laham, M. A.; Peng, C. Y.; Nanayakkara, A.; Challacombe, M.; Gill, P. M. W.; Johnson, B.; Chen, W.; Wong, M. W.; Gonzalez, C.; Pople, J. A. *Gaussian 03*, revision C.02; Gaussian, Inc.: Pittsbourgh, PA, 2003.
(47) Becke, A. D.; Yarkony, D. R. In *Modern Electronic Structure Theory Part II*; World Scientific: Singapore, 1995.
(48) Hehre, W. J.; Radom, L.; Schleyer, P. v. R.; Pople, J. A. *Ab Initio Molecular Orbital Theory*; John Wiley & Sons: New York, 1986.
(49) Hay, P. J.; Wadt, W. R. *J. Chem. Phys.* **1985**, *82*, 270.
(50) Wadt, W. R.; Hay, P. J. *J. Chem. Phys.* **1985**, *82*, 284.
(51) Hay, P. J.; Wadt, W. R. *J. Chem. Phys.* **1985**, *82*, 299.
(52) Harris, D. L. *Curr. Opin. Chem. Biol.* **2001**, *5*, 724.
(53) Noodleman, L.; Lovell, T.; Han, W.-G.; Li, J.; Himo, F. *Chem. Rev.* **2004**, *104*, 459.
(54) Solomon, E. I.; Szilagyi, R. K.; DeBeer, George, S.; Basumallick, L. *Chem. Rev.* **2004**, *104*, 419.
(55) Foresman, J. B.; Keith, T. A.; Wiberg, K. B.; Snoonian, J.; Frisch, M. J. *J. Phys. Chem.* **1996**, *100*, 16098.
(56) Jabri, E.; Carr, M. B.; Hausinger, R. P.; Karplus, P. A. *Science* **1995**, *268*, 998.
(57) Jabri, E.; Karplus, A. *Biochemistry* **1996**, *35*, 10616.
(58) Case, D. A.; Darden, T. A.; Cheatham, T. E., III; Simmerling, C. L.; Wang, J.; Duke, R. E.; Luo, R.; Merz, K. M.; Wang, B.; Pearlman, D. A. Crowley, M.; Brozell, S.; Tsui, V.; Gohike, H.; Mongan, J.; Hornak, V.; Cui, G.; Beroza, P.; Schafmeister, C.; Caldwell, J. W.; Ross, W. S.; Kollman, P. A. *Amber 8*; University of California, San Francisco, 2004.
(59) Estiu, G. L.; Merz, K. M., Jr. *J. Am. Chem. Soc.* **2004**, *126*, 11832.
(60) Basner, J. E.; Schwartz, S. D. *J. Am. Chem. Soc.* **2005**, *127*, 13822.
(61) Blakeley, R. L.; Treston, A.; Andrews, R. K.; Zerner, B. *J. Am. Chem. Soc.* **1982**, *104*, 612.
(62) Marlier, J. F.; Cleland, W. W. *Biochemistry* **2006**, *45*, 9940.